ATOMIC IODINE GENERATION VIA FLUORINE ATOMS FOR CHEMICAL OXYGEN–IODINE LASER

Miroslav ČENSKÝ[a1,*], Otomar ŠPALEK[a2], Vít JIRÁSEK[a3], Jarmila KODYMOVÁ[a4] and Ivo JAKUBEC[b]

[a] *Institute of Physics, Academy of Sciences of the Czech Republic, Na Slovance 2, 182 21 Prague 8, Czech Republic; e-mail: [1] censky@fzu.cz, [2] spaleko@fzu.cz, [3] jirasek@fzu.cz, [4] kodym@fzu.cz*

[b] *Institute of Inorganic Chemistry, Academy of Sciences of the Czech Republic, 250 68 Řež near Prague, Czech Republic; e-mail: jakubec@iic.cas.cz*

Received September 26, 2005
Accepted December 22, 2005

Chemical generation of atomic iodine for a chemical oxygen–iodine laser (COIL) was investigated experimentally. In the two-step reaction mechanism, molecular fluorine reacts with nitrogen oxide and formed fluorine atoms react then with hydrogen iodide to iodine atoms. The efficiency of this process was studied in dependence on mixing conditions, flow rate of reacting gases and pressure in reactor. A maximum concentration of atomic iodine was obtained at approximately equimolar ratio of reacting gases (F_2, NO and HI), which agrees well with the stoichiometry of production reactions. A shortage of any reacting gases limits the rate of atomic iodine formation. An excess of F_2 relative to NO at a simultaneous deficiency of HI had a most detrimental effect on atomic iodine production. High concentrations of atomic iodine (5–8 × 10^{15} cm^{-3}) were achieved by this method at pressures 4–9 kPa, which are sufficient for a COIL operation. This makes it possible to use the above method as a source of iodine atoms and their injection into the primary flow of singlet oxygen in COIL.

Keywords: Atomic iodine; Atomic fluorine; Halogens; NO; Chemical oxygen–iodine laser; COIL; Kinetics.

A chemical oxygen–iodine laser (COIL) radiates in the near infrared region due to stimulated emission on the 3–4 transition in iodine atom.

$$I(^2P_{1/2}) \rightarrow I(^2P_{3/2}) + h\nu\ (1.315\ \mu m) \qquad (1)$$

Atomic iodine is conventionally generated by dissociation of molecular iodine evaporated from the solid or liquid state. The I_2 dissociation consumes the energy of several molecules of singlet oxygen, $O_2(^1\Delta_g)$, per one iodine molecule.

$$I_2 + n\ O_2(^1\Delta_g) \rightarrow 2\ I + n\ O_2(^3\Sigma_g) \qquad n = 4–6 \qquad (2)$$

Collect. Czech. Chem. Commun. 2006, Vol. 71, No. 5, pp. 739–755

doi:10.1135/cccc20060739

This fraction of $O_2(^1\Delta_g)$ energy is therefore lost and cannot be utilized for the laser pumping reaction (the rate constants are given below in cm^3 $molecule^{-1}$ s^{-1} or cm^6 $molecule^{-2}$ s^{-1}).

$$O_2(^1\Delta_g) + I(^2P_{3/2}) \rightarrow O_2(^3\Sigma_g) + I(^2P_{1/2}) \qquad k_3 = 7.8 \times 10^{-11} \qquad (3)$$

Employing another way of atomic iodine production can avoid this energy loss. This way could further eliminate a fast quenching of excited iodine atoms (denoted hereafter I*) by I_2 molecules

$$I(^2P_{1/2}) + I_2 \rightarrow I(^2P_{3/2}) + I_2 \qquad k_4 = 3.1 \times 10^{-11} \qquad (4)$$

and also solve problems with controlling the rate of I_2 evaporation, I_2 concentration measurement, and heating the whole I_2 delivery system. Injection of I atoms instead of I_2 can also result in more homogeneous laser gain medium. In an effort to suppress or avoid the mentioned drawbacks of the conventional iodine scheme in COIL, several alternative methods of atomic iodine generation have been explored. The I_2 dissociation in microwave discharge was studied by Endo et al.[1], who estimated a laser power enhancement by 9% using transonic injection of pre-dissociated iodine into the primary flow of $O_2(^1\Delta_g)$. Subsonic or supersonic mixing of $O_2(^1\Delta_g)$ with predissociated iodine brought no positive effect. Some improvement of iodine dissociation (up to 50%) and laser power enhancement was achieved with hybrid iodine injector combined with mw cavity[2]. A higher degree of I_2 dissociation (up to 80%) could be provided using a radiofrequency discharge, however, at the expense of high energy consumption (5–10 kW $mmol^{-1}$ I_2) and consecutive substantial gas heating[3]. Moreover, the described methods do not avoid the mentioned problems with handling the I_2 vapor. The dissociation of alkyl iodide (RI) in the glow discharge was also studied and the yield of iodine atoms of 30–40% was achieved[4].

A chemical method of atomic iodine generation for a COIL was proposed and developed in our laboratory[5–7], which is based on the reaction of gaseous hydrogen iodide with atomic chlorine formed in a previous fast reaction of chlorine dioxide with nitrogen oxide. First studies of this reaction system in nitrogen flow were performed using small-scale reactors, which gave after optimization a high yield of atomic iodine (up to 80–100% relative to ClO_2). Similar results were obtained in COIL with mixing the reacting gases into primary flow of nitrogen-helium mixture upstream the supersonic nozzle throat. The small-signal gain of 0.4 % cm^{-1} and the laser output power of 450 W were attained in COIL with sequential admixing

the reacting gases into the primary flow of $O_2(^1\Delta_g)$ upstream the supersonic nozzle[8]. The chemical efficiency of the COIL operated in this set-up (≤13%) was limited most probably due to the partial $O_2(^1\Delta_g)$ quenching by $HO_2^{\bullet}$ radical formed in the reaction of HI with $O_2(^1\Delta_g)$. A significant $O_2(^1\Delta_g)$ quenching was proved experimentally when only HI was mixed with $O_2(^1\Delta_g)$. A separate generation of atomic iodine in the side reactors is studied presently, followed by I atoms injection into the primary $O_2(^1\Delta_g)$ stream in COIL. The developed method of atomic iodine generation via Cl atoms has a drawback of the on-site preparation of gaseous chlorine dioxide from chlorine and $NaClO_2$ solution since this gas cannot be prepared in advance and pressurized to cylinders. Therefore another chemical method of atomic iodine production via atomic fluorine has been investigated using only the gas reaction system. This paper concerns the results of this study.

REACTION KINETICS

The atomic iodine production proceeds in a two-step reaction process. In the first step, atomic fluorine is formed in the reaction of nitrogen oxide with molecular fluorine[9–11].

$$NO + F_2 \rightarrow NOF + F \qquad k_5 = 7 \times 10^{-13} \exp(-1150/T) \qquad (5)$$

In the second step, the formed fluorine atoms react with hydrogen iodide to atomic iodine[12,13].

$$F + HI \rightarrow HF + I(^2P_{3/2}) \qquad k_6 = 1.5 \times 10^{-10} \exp(-5057.8/RT) \qquad (6)$$

Several loss-processes accompany F atoms formation[12,14,15].

$$F + NO + NO \rightarrow NOF + NO \qquad k_7 = 1.7 \times 10^{-31} \qquad (7)$$

$$F + NO + N_2 \rightarrow NOF + N_2 \qquad k_8 = 1.1 \times 10^{-31} \qquad (8)$$

$$F + F + N_2 \rightarrow F_2 + N_2 \qquad k_9 = 1.02 \times 10^{-37} T^{1.5} \qquad (9)$$

$$F + F + \text{wall} \rightarrow F_2 + \text{wall} \qquad \gamma_{10} = 0.05 \qquad (10)$$

$$F + I_2 \rightarrow IF + I \qquad k_{11} = 4.3 \times 10^{-10} \qquad (11)$$

Atomic iodine may be partially lost in ternary reactions with other molecules[16,17]

$$I + I + N_2 \rightarrow I_2 + N_2 \qquad k_{12} = 6.15 \times 10^{-4}(T/298)^{0.07} \exp(7433/RT) \qquad (12)$$

$$I + I + I_2 \rightarrow I_2 + I_2 \qquad k_{13} = 2.68 \times 10^{-31}(T/298)^{-3.06} \exp(6568/RT) \qquad (13)$$

$$I + I + HI \rightarrow I_2 + HI \qquad k_{14} = 8.13 \times 10^{-32}(T/298)^{-3.5} \qquad (14)$$

$$I + NO + N_2 \rightarrow INO + N_2 \qquad k_{15} = 1.8 \times 10^{-32}(T/298)^{-1} \qquad (15)$$

and in the reaction with formed INO [18].

$$I + INO \rightarrow I_2 + NO \qquad k_{16} = 1.66 \times 10^{-10} \qquad (16)$$

Iodine atoms can also react with molecular fluorine and recombine on the walls[19]

$$I + F_2 \rightarrow IF + F \qquad k_{17} = 1.9 \times 10^{-14} \qquad (17)$$

$$I + I + \text{wall} \rightarrow I_2 + \text{wall} \qquad \gamma_{18} = 1.0 \qquad (18)$$

where γ is the striking coefficient. The above given reactions are strongly exothermic. The reaction enthalpies of the main production reactions are: $\Delta H_5 = -77$ kJ mol^{-1}, $\Delta H_6 = -230$ kJ mol^{-1}, $\Delta H_{7,8} = -236$ kJ mol^{-1}, and $\Delta H_{17} = -130$ kJ mol^{-1}. The enthalpy of reaction (*6*) was calculated with respect to the vibrational distribution of HF molecules formed in this reaction[12].

EXPERIMENTAL

Two small-scale reactors were employed during the experimental investigation of this reaction system. A cross-section of the reactor 1 is schematically shown in Fig. 1. This reactor is made of stainless steel tube of 10 mm i.d. Two injectors are inserted in the reactor bends for admixing the secondary gases (10% NO in mixture with N_2, and 10% HI in N_2) into the primary gas flow (10% F_2 in N_2). Either position 1 or 2 of NO injector 1 was used. The HI/N_2 mixture was introduced through injector 3. The injectors were made of stainless-steel tube of 5 mm o.d. with two or three rows of openings drilled perpendicularly to injector axis at a distance of 1–3 mm from the injector end. The NO injector had 24 openings of 0.4 mm i.d., and the HI injector had 16 openings of the same diameter. A gas exiting the reactor entered the first detection cell after cca 0.027 ms, and the second detection cell after 2.7 ms. Both detection cells were longitudinally flown tubes of 8 mm i.d. and 50 mm long with glass

windows on both ends. Atomic iodine concentration was measured in these cells by the iodine scan diagnostics (ISD)[20]. This diagnostics is based on the near IR spectroscopy using a narrow-band tunable diode probe laser, which monitors a gain or absorption on the I*–I transition at 1.315 μm. Gas temperature was calculated from the Gaussian full width after deconvolution of the Voigt profile of the measured absorption–frequency curve.

A cross-section of reactor 2 is shown in Fig. 2. The reactor consisted of rectangular reaction space (25 mm wide and 8 mm high) with a delta-shaped channel for introducing the primary gas (10% F_2 in N_2). The NO injector was inserted in the cavity center perpendicularly to the primary gas flow, and two HI injectors were embedded in the upper and bottom walls of the cavity. The NO injector 3 contained two rows of holes of 0.4 mm i.d. (arranged in lines) with 23 holes in each row. The distance between adjacent holes was 1 mm. Both rows of holes were oriented in vertical direction (up and down). Each HI injector 4 contained 9 holes of 0.4 mm i.d. in one row. A time delay between NO and HI injection could be varied to a certain extent by turning the injectors 4. In some experiments, the order of NO and HI injection was reversed, (HI was inlet into the injector 3 and NO was introduced

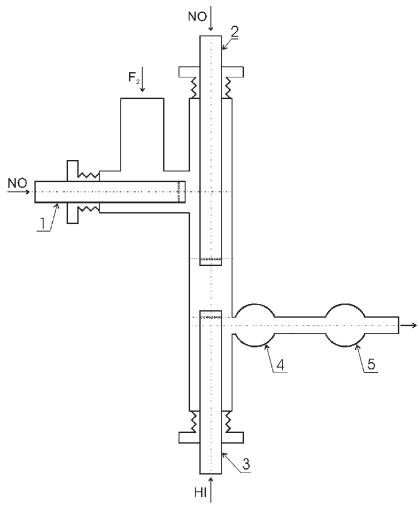

FIG. 1
Cross-section of longitudinal flow reactor with axially movable NO and HI injectors: 1, NO injector (position 1); 2, NO injector (position 2); 3, HI injector; 4, first detection cell; 5, second detection cell

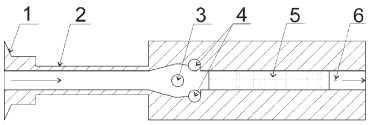

FIG. 2
Cross-section of transverse flow reactor: 1, input flange; 2, delta-shaped channel; 3, injector for first secondary gas (NO or HI); 4, injectors for second secondary gas; 5, optical cavity for atomic I detection; 6, thermocouple

into the injector 4). The second part of the rectangular cavity with two side windows served for ISD detection of atomic iodine. The probe beam passed through the wedge-shaped windows of the cell perpendicularly to the gas flow. The windows were coated with a thin layer of Teflon in order to protect glass against HF. The probe beam emitter/detector unit was mounted on the assembly of motorized linear positioning equipment controlled by PC. In this configuration, the probe beam could move along the cell on the path within the 12 and 60 mm distance from the axis of the second gas injector (dotted area in Fig. 2). The probe beam moved at a velocity of 4 mm s^{-1} in the duct axis. The gas temperature was measured with a jacketed Ni–CrNi thermocouple 6 (1 mm o.d.), which was inserted perpendicularly to the gas flow, 5 mm downstream from the end of the windows.

The gas exiting the reactor was exhausted with a rotary pump (capacity 25 m^3 h^{-1}) through a liquid nitrogen trap, where most NOF, IF, HI, NO, and I_2 was frozen. The rotary pump operated with a special oil NC 1/14 (Leybold Ltd., Germany) consisting of perfluorinated polyether, which is chemically inert to fluorine. The residual F_2 in the exhausting gas was then absorbed in the column filled with aluminosilicates.

A local flow rate of atomic iodine n_I (in μmol s^{-1}) was calculated from a local concentration of atomic iodine, c_I, evaluated from the ISD data for the central line of the gas channel. Equation (*19*) was used for this calculation

$$n_I = c_I V/N_A \qquad (19)$$

where N_A is the Avogadro constant and V is a volume flow rate of gas mixture through the detection cell. This was evaluated from the modified equation of state

$$V = n_t RT/P \qquad (20)$$

where n_t is the total molar flow rate representing the sum of molar flow rates of all gas components, T is the gas temperature, and P is the pressure measured in the detection cell.

RESULTS AND DISCUSSION

Measurements with the Longitudinal Flow Reactor

Effects of Flow Rates of Reacting Gases with NO–HI Injection Order

The NO/N_2 mixture (50–300 μmol s^{-1} NO) was introduced through the injector 1 or 2 in Fig. 1 into the primary F_2/N_2 flow (60–260 μmol s^{-1} F_2), and HI/N_2 mixture through the injector 3 (60–450 μmol s^{-1} HI). Time intervals were 0.027 ms between NO and HI admixing, and 2.7 ms between HI injection and first detection cell of atomic iodine. Total pressure in the reactor was 1.5–3 kPa.

First experiments were performed with a very short delay between NO and HI injection into the F_2/N_2 flow (0.023 ms). Examples of measured rate of atomic iodine production in dependence on F_2, NO, and HI flow rates, respectively, are shown in Figs 3–5. Experimental data in these figures were

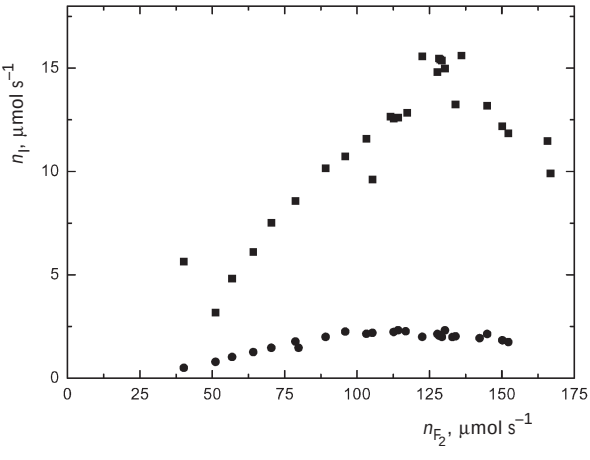

FIG. 3
Flow rate of atomic iodine in dependence on F_2 flow rate; 141 μmol s^{-1} NO and 82 μmol s^{-1} HI; τ_{NO-HI} = 0.027 ms; ■ 1st detection cell, τ_{HI-ISD} = 2.7 ms; ● 2nd detection cell, τ_{HI-ISD} = 10 ms

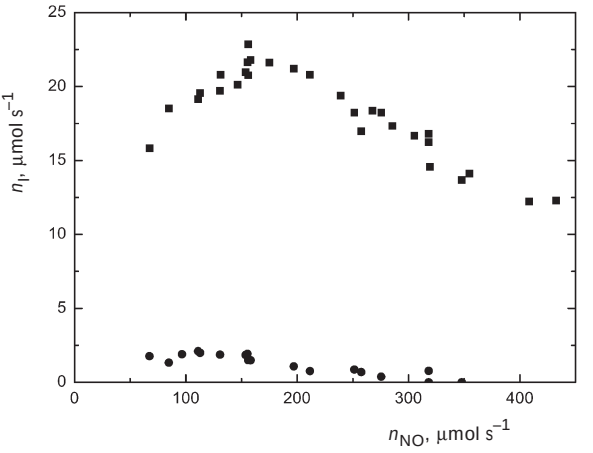

FIG. 4
Flow rate of atomic iodine in dependence on NO flow rate; 155 μmol s^{-1} F_2, 146 μmol s^{-1} HI; other conditions the same as in Fig. 3

recorded simultaneously in the first detection cell (τ_{HI-ISD} = 2.7 ms) and the second detection cell (τ_{HI-ISD} = 10 ms). The flow rate of iodine atoms initially increased with increasing F_2 flow rate (Fig. 3) obviously due to enhancement of the reaction rate (*5*). The following decline was explained by consumption of I atoms in their reaction with F_2 molecules (*17*). Atomic fluorine formed in reaction (*17*) could produce further atomic iodine by reaction (*6*) provided that HI is in sufficient concentration. This was proved by the experiment at 2.8 times higher HI flow rate (with the same NO), in which no decrease in I flow rate was observed with increasing F_2 flow rate. The initial increase in atomic I production with the NO flow rate (Fig. 4) was ascribed to acceleration of reaction (*5*). The following decrease reflects probably an increasing effect of the loss-reactions (*7*) and (*8*). A maximum production of atomic I was attained in a rather wide range of the NO/F_2 ratio of molar flow rates (from 0.8 to 2.3). This is probably caused by the simultaneous effect of the NO flow rate on the F formation rate, and a shift of the reaction region closer to the NO injector with increasing NO flow rate. The dependence of atomic iodine production on the HI flow rate (Fig. 5) was similar to the previous dependences. The increasing HI flow rate in Fig. 5 obviously first accelerated the reaction (*6*). The following decrease could be caused by shifting the region of maximum production of atomic iodine closer to the HI injection. This explanation was supported by much lower concentration of atomic iodine recorded in the second cell.

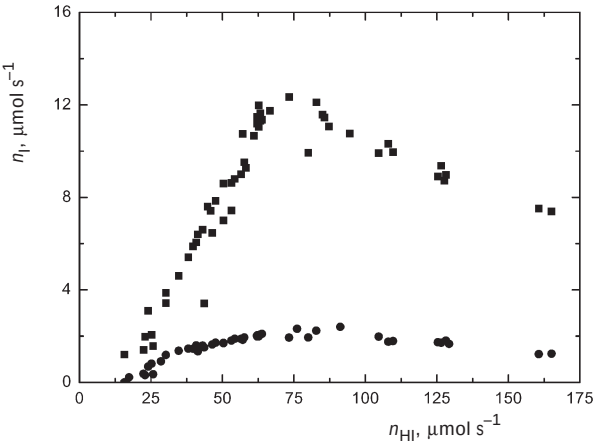

FIG. 5
Flow rate of atomic iodine in dependence on HI flow rate; 105 μmol s^{-1} F_2, 141 μmol s^{-1} NO; other conditions the same as in Fig. 3

Effects of Time Interval Between NO and HI Injection

The effect of the time interval between NO and HI injection was studied in experiments with different positions of NO and HI injectors. In measurements with a NO–HI interval of 0.23 ms, nearly identical data with those at the interval of 0.027 ms were obtained, and no significant effect was observed even when this interval was prolonged up to 0.34 ms. Only when this interval was prolonged to 1.45 ms, the I atoms production decreased by 5 to 30%. According to the 1-D modeling including reactions (*5*) and (*7*)–(*9*), the concentration of F atoms should grow still up to ~3 ms, when the effect of loss reactions starts to prevail[22].

Figure 6 illustrates the effect of the time interval between the HI injection and atomic I detection on the atomic iodine flow rate. It documents stability of I atoms in the reaction mixture. It can be seen that the flow rate of I atoms was significantly lower when this time interval increased from 2.1 to 2.7 ms. The flow rates of I atoms measured in the second detection cell (corresponding to a time interval 9.4 or 10 ms) were several times lower, which reveals a strong effect of the loss reactions, mainly (*15*) and (*16*).

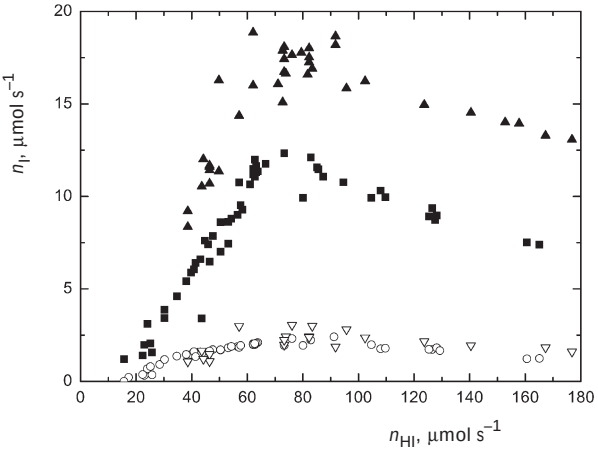

FIG. 6
Flow rate of atomic iodine in dependence on HI flow rate and for different time intervals between HI injection and atomic I detection; τ_{HI-ISD} (ms): 2.1 (▲), 2.7 (■), 9.4 (▽), 10 (○); 109 μmol s^{-1} F_2, 142 μmol s^{-1} NO

Measurements with the Rectangular Reactor

NO–HI Injection Order

A more detailed study was performed with the rectangular reactor 2 and movable ISD beam. A downstream or upstream direction of the probe beam movement along the gas flow had no effect on the measured iodine concentration. Figure 7 shows the effect of F_2 flow rate on the concentration profile of atomic iodine along the gas flow. The iodine concentration was about twice higher when the F_2 flow rate increased 2.7 times, i.e. from 52 to 159 μmol s^{-1}. With further increasing the F_2 flow rate, the concentration of atomic iodine was nearly the same at the beginning of the optical cell but then declined with distance. This may be ascribed to a detrimental effect of reaction (*17*) consuming I atoms at F_2 excess. Contrary to this result, no significant decrease in I concentration with distance was observed at a higher HI flow rate (300 μmol s^{-1}) and nearly the same F_2 and NO flow rates. This can be explained by additional formation of iodine atoms in the reaction of excess HI and F atoms formed in reaction (*17*).

Figure 8 shows the effect of the NO flow rate at the molar flow rate ratio F_2:NO:HI = 1:*X*:0.82, with *X* = 0.65–3. No substantial effect of the NO flow rate was found for the ratio between 1.1 and 2.3. The iodine concentration

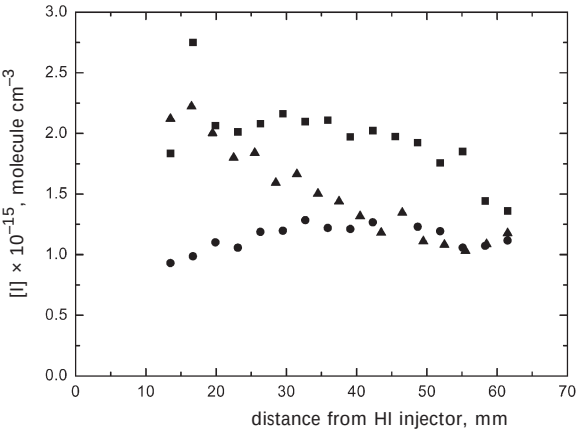

FIG. 7
Concentration of atomic iodine along gas flow at NO–HI injection order; 221 μmol s^{-1} NO, 134 μmol s^{-1} HI; F_2 flow rate (μmol s^{-1}): 58 (●), 159 (■), 277 (▲); τ_{NO-HI} = 0.18 ms, τ_{HI-ISD} = 0.45–2 ms; *p* = 1.5–2.1 kPa

was not significantly lower when the NO/F_2 flow ratio was only 0.65. A lower iodine concentration, however, was measured at a still greater deficiency of NO relative to F_2. A substantial excess of NO over F_2 caused only a small decrease in iodine concentration, which can be ascribed to the effect of loss reactions (*7*) and (*8*). The effect of HI flow rate on iodine concentration is shown in Fig. 9. This figure shows that the iodine concentration first increases substantially with increasing HI flow rate, but a substantial excess of HI vs F_2 and NO enhanced the iodine concentration only slightly. This behavior indicates a "titration" of F atoms by HI.

HI–NO Injection Order

The HI–NO order of secondary gases injection into the primary F_2 flow was proposed with the aim to reduce effects of loss-reactions (*7*)–(*10*) competing with the production reaction (*6*). An example of the effect of F_2 flow rate on atomic iodine generation in this configuration is shown in Fig. 10. The maximum of iodine concentration was shifted with increasing F_2 flow rate in the upstream direction. This reflects acceleration of both production and loss reactions with increasing concentration of fluorine. The effect of HI flow rate on I production at excess F_2 relative to NO (NO/F_2 = 0.58) and HI is shown in Fig. 11. The iodine concentration initially increased with in-

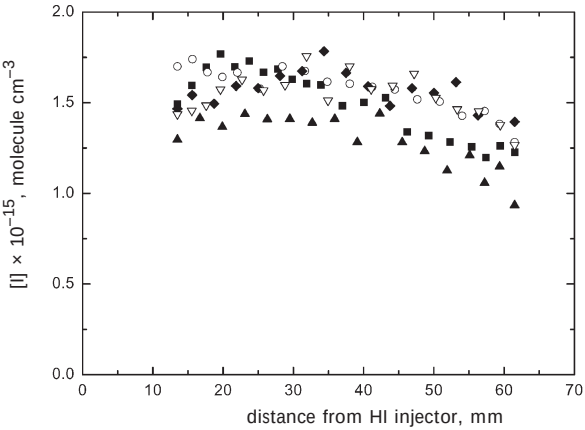

FIG. 8
Concentration of atomic iodine along gas flow at NO–HI injection order; 159 μmol s^{-1} F_2, 130 μmol s^{-1} HI; NO flow rate (μmol s^{-1}): 104 (■), 172 (○), 306 (◆), 371 (▽), 486 (▲); p = 1.5–2.5 kPa; other data as in Fig. 7

creasing distance from NO injector regardless of the HI flow rate. This obviously copied the increasing concentration of F atoms with time. The iodine concentration then began to decrease probably because of HI exhaustion, and subsequent increasing loss of I atoms mostly due to reaction (*17*). This

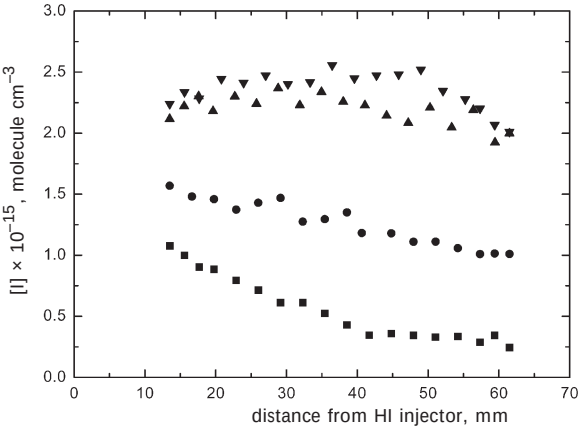

FIG. 9
Concentration of atomic iodine along gas flow at NO–HI injection order; 186 μmol s^{-1} F_2, 181 μmol s^{-1} NO; HI flow rate (μmol s^{-1}): 61 (■), 128 (●), 225 (▲), 472 (▼); other data as in Fig. 7

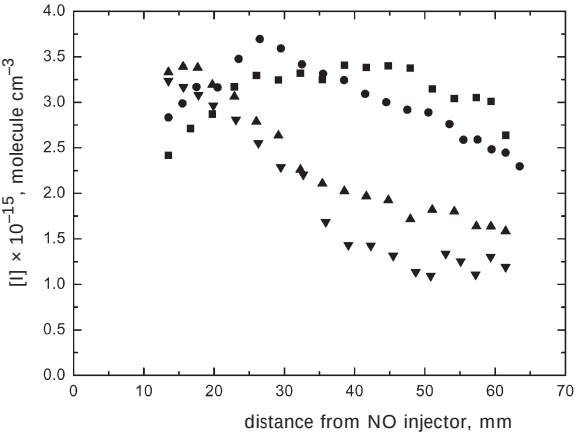

FIG. 10
Concentration of atomic iodine along gas flow at HI–NO injection order; 94 μmol s^{-1} HI, 381 μmol s^{-1} NO; F_2 flow rate (μmol s^{-1}): 153 (■), 195 (●), 267 (▲), 343 (▼); τ_{HI-NO} = 0.18 ms, τ_{NO-ISD} = 0.45–2 ms; p = 2.35–2.8 kPa

effect was suppressed at higher HI flow rates due to additional formation of iodine atoms from F atoms produced in reaction (*17*). In the measurements with HI–NO injection sequence, nearly twice-higher rate of atomic iodine production was attained at similar flow rates of reactants. This can be explained by a higher loss of F atoms in the NO–HI sequence of injection. This loss via reactions (*7*), (*8*), (*15*) and (*16*) takes place mostly at the boundary between NO jet and primary flow with F_2, where a local excess of F atoms and insufficient HI concentration exist. In the HI–NO order, HI is premixed with F_2 upstream the NO injector and thus is more available to F atoms in the regions of their formation.

A total pressure in the above measurements was up to 3 kPa only. This pressure is too low to inject either atomic fluorine or iodine into the primary flow upstream the supersonic nozzle throat in COIL. Further experiments were therefore performed at higher pressures (mostly between 4–9 kPa), which were attained at higher flow rates. Figure 12 shows an example of the dependence of iodine concentration on HI flow rate at the ratio NO/F_2 equal to ca. 1. At the lowest HI flow, a substantial decrease in iodine concentration with time (or with distance) was mostly caused by reaction (*17*). At higher HI flow rates, this effect was suppressed (see the above explanation).

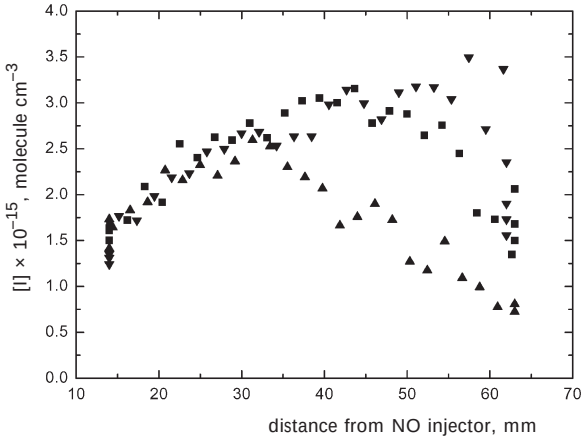

FIG. 11
Concentration of atomic iodine along gas flow at HI–NO injection order; 378 μmol s^{-1} F_2, 213 μmol s^{-1} NO; HI flow rate (μmol s^{-1}): 148 (▲), 266 (■), 316 (▼); p = 2.5–3 kPa; time intervals as in Fig. 10

In these measurements, the yield of atomic iodine relative to F_2 ranged from 13 to 27%, the yield related to HI was between 25 and 50%. It was generally lower at higher total pressures. This is obviously due to the fact that the production processes are bimolecular reactions (*5*), (*6*), whereas the loss-processes are mostly ternary reactions (*7*)–(*9*), (*12*)–(*15*). An improvement of yield is anticipated in the system with a lower fraction of diluting gas. This should increase the temperature and also reduce the rate of ternary loss-reactions involving nitrogen. A higher temperature increases rate constants of the main production reactions (*5*), (*6*) and reduces rate constants of ternary loss-reactions (*13*)–(*15*).

Temperature of Reaction Mixture

Temperature of the reaction mixture was measured with a thermocouple (see Fig. 2) and also calculated from the shape of the absorption–frequency curves recorded during ISD measurements. The first method suffered from a rather long time response (tens of seconds), and ISD data were rather scattered. Nevertheless, the temperature data from both methods were in a reasonable agreement. The temperature measured at lower flow rates and pressures (up to 3 kPa) was between 300 and 400 K. Gas temperature was higher at higher flow rates and pressure, e.g. between 400 and 700 K for conditions given in the caption of Fig. 12. The temperature increase was caused by exothermic reactions occurring in the studied system.

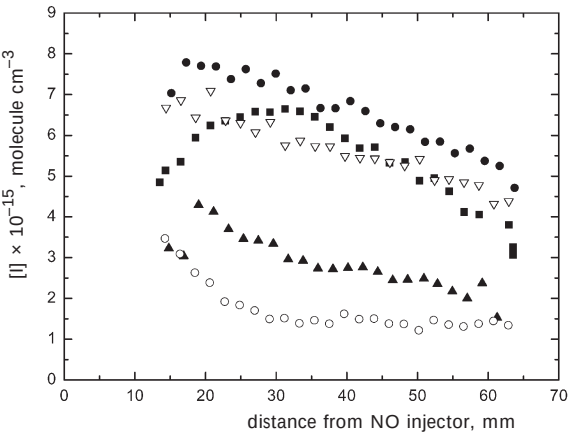

FIG. 12

Concentration of atomic iodine along gas flow at HI–NO injection order; 892 μmol s^{-1} F_2, 932 μmol s^{-1} NO; HI flow rate (μmol s^{-1}): 309 (○), 380 (▲), 489 (■), 506 (▽), 635 (●); p = 7.4–9.2 kPa; time intervals as in Fig. 10

Applicability of This Method to COIL

This experimental study has shown that the proposed method can produce atomic iodine in concentrations sufficient for operation of a supersonic COIL. The experimental results and modeling showed that the reactant mixing scheme employed in the Cl → I system, i.e. admixing of reactants into primary $O_2(^1\Delta_g)$ flow upstream the nozzle throat in COIL [8], cannot be applied in the F → I system. The main reason is that rather slow formation of F atoms followed by I atoms generation would be accompanied by fast pumping of I atoms and following quenching of I* atoms in the $O_2(^1\Delta_g)$ flow. The main quenchers of I* in this system are water (k_{H2O} = 2 × 10^{-12} cm^3 $molecule^{-1}$ s^{-1})[21] and HF molecules (k_{HF} = 2.8 × 10^{-12} cm^3 $molecule^{-1}$ s^{-1})[22]. The latter process can be avoided by using deuterium iodide, DI, instead of HI. In the described arrangement a rather fast reaction of F atoms with water (k = 4.15 × 10^{-11} exp (–400/T) cm^3 $molecule^{-1}$ s^{-1})[23] could also compete with the atomic iodine production (*6*). These problems could be avoided by using separate reactors for atomic iodine production and following injection of atomic iodine into the main $O_2(^1\Delta_g)$ flow. Further investigation is currently devoted to development of this system.

CONCLUSIONS

1. The chemical generation of atomic iodine via F atoms was investigated experimentally. Sufficiently high concentrations of atomic iodine (5–8 × 10^{15} cm^{-3}) can be achieved by this method even at pressures 4–9 kPa that make possible to inject the gas with iodine atoms into the singlet oxygen flow in the chemical oxygen–iodine laser.

2. The maximum concentration of atomic iodine was attained with reacting gases (F_2, NO and HI) at approximately equimolar ratio, which agrees with the stoichiometry of production reactions. A shortage of any reacting gases limits the rate of atomic iodine formation. A considerable excess of F_2 over NO at simultaneous deficient HI flow is detrimental due to the loss of I atoms by reaction (*17*). At sufficient HI flow, this negative effect was compensated by additional formation of atomic iodine through the reaction of residual HI with F atoms formed in reaction (*17*). A substantial excess of NO over F_2 caused only a small decrease in I concentration, which could be ascribed to the effect of loss-reactions (*7*) and (*8*).

3. The atomic iodine production was affected by the order of injection of secondary gases (NO and HI). A higher rate of I production was attained

when HI was injected first and NO as the second gas into the primary gas flow containing fluorine.

4. The temperature of reaction mixture ranged from 320 to 700 K, and was increasing with increasing flow rates of all reacting gases.

5. A maximum yield of atomic iodine related to F_2 flow rate was 27%, a maximum I yield relative to HI was 51%. An improvement is anticipated in a system with a lower fraction of diluting gas.

6. A COIL configuration with chemical production of atomic iodine was proposed based on obtained experimental results and theoretical modeling of this reaction system.

The USAF European Office for Research and Development (grant No. FA8655-02-M4040) and the Grant Agency of the Czech Republic (grants No. 202/05/0359 and No. 203/02/D061) supported this work.

REFERENCES

1. Endo M., Sugimoto D., Okamoto H., Nanri K., Uchiama T., Takeda S., Fujioka T.: *Jpn. J. Appl. Phys.* **2000**, *39*, 468.
2. Okamoto H., Hirata T., Shinoda K., Sugimoto D., Endo M., Fujioka T., Takeda S.: *Proc. 31st Plasmadynamics and Lasers Conference, Denver, Colorado, 2000*. Paper No. AIAA-2000-2492. AIAA, Reston, Virginia, USA, 2000.
3. Quillen B., Schall W.: *CD Proceedings of COIL R&D Workshop, Stuttgart, Germany, 2003*. DLR Stuttgart, Germany, 2003.
4. Mikheyev P. A., Shepelenko A. A., Voronov A. V., Kupryaev N. V.: *Russian J. Quantum Electron.* **2002**, *32*, 1.
5. Špalek O., Jirásek V., Kodymová J., Jakubec I., Čenský M.: *Proc. SPIE* **2000**, *4184*, 111.
6. Jirásek V., Špalek O., Kodymová J., Čenský M.: *Chem. Phys.* **2001**, *269*, 167.
7. Špalek O., Jirásek V., Čenský M., Kodymová J., Jakubec I., Hager G. D.: *Chem. Phys.* **2002**, *282*, 147.
8. Špalek O., Čenský M., Jirásek V., Kodymová J., Jakubec I., Hager G. D.: *IEEE J. Quantum Electron.* **2004**, *40*, 564.
9. Johnston S., Bertin H. J.: *J. Am. Chem. Soc.* **1959**, *81*, 6402.
10. Kolb C. E.: *J. Chem. Phys.* **1976**, *64*, 3087.
11. Pollock T. L., Jones W. E.: *Can. J. Chem.* **1973**, *51*, 2041.
12. Jonathan N., Melliar-Smith C. M., Okuda S., Slater D. H., Timlin D.: *Mol. Phys.* **1971**, *22*, 561.
13. Sung J. P., Setser D. V.: *Chem. Phys. Lett.* **1977**, *48*, 413.
14. Jones W. E., Skolnik E. G.: *Chem. Rev.* **1976**, *76*, 563.
15. Kim P., McLean D. I., Valance W. G.: Abstracts of the *164th National Meeting Am. Chem. Soc., New York, 1972*.
16. Yang T. T., Copeland D. A., Bauer A. H., Quan V., McDermott W. E., Cover R. A., Smith D. M.: *28th Plasmadynamics and Laser Conference, Atlanta, 1997*. Paper No. AIAA-1997-2384. AIAA, Reston, Virginia, USA, 1997.

17. Bemand P. P., Clyne M. A. A. A., Watson R. T.: *J. Chem. Soc., Faraday Trans. 1* **1973**, *69*, 1356.
18. Van den Bergh H., Troe J.: *J. Chem. Phys.* **1976**, *64*, 736.
19. Manke G. C., Jr., Henshaw T. L., Madden T. J., Herbelin J. M., Rafferty B. D, Hager G. D.: *AIAA J.* **2001**, *39*, 447.
20. Tate R. F., Hunt B. S., Helms C. A, Truesdell K. A., Hager G. D.: *IEEE J. Quantum Electron.* **1995**, *31*, 1632.
21. Burde D. H., McFarlane R. A.: *J. Chem. Phys.* **1976**, *64*, 1850.
22. Coombe J., Pritt J.: *J. Chem. Phys.* **1977**, *66*, 5214.
23. Walther C. D., Wagner H. G.: *Ber. Bunsenges. Phys. Chem.* **1983**, *87*, 403.